account the fall time (90 ps) of the drive current, the fall time of the laser was estimated to be 80 ps. The cutoff frequency is obtained from the fall time by $f_c = \ln 9/(2\pi t_f)$. Substituting 80 ps for t_f, a cutoff frequency of 4·4 GHz was obtained, and this deduced value is in fairly good agreement with the measured value (4·3 GHz).

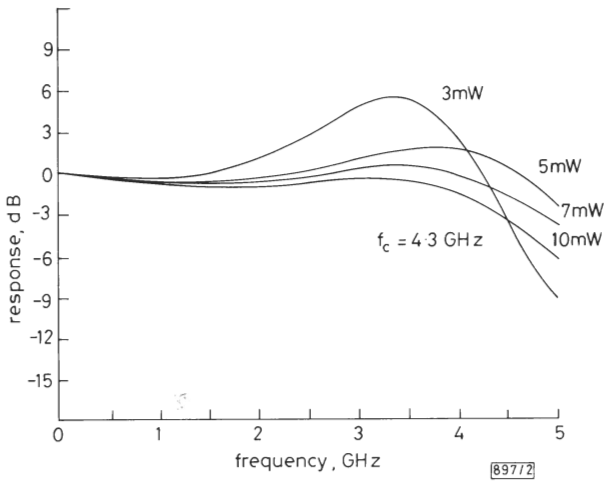

Fig. 2 *Small-signal responses of modified DFB-PPIBH laser at various bias levels*

Since the fall time of the modified DFB-PPIBH laser is shorter than 100 ps, multigigabit operation is expected using this laser. Fig. 4 shows the output signal of the modified DFB-PPIBH laser under 5 Gbit/s non-return-to-zero (NRZ) modulation. As shown in the Figure, a good eye pattern was obtained.

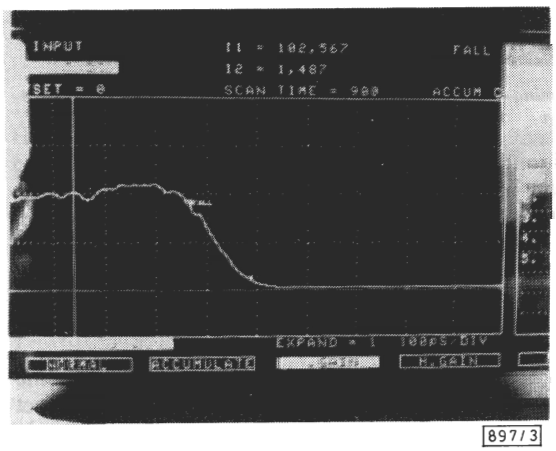

Fig. 3 *Output signal under pulsed operation of modified DFB-PPIBH laser*

Discussion: The value of f_c deduced from the fall time is in good agreement with the measured f_c. However, the predicted f_c is slightly smaller than the measured f_c. The discrepancy is explained as follows. We calculated the capacitance associated the *pn* junctions of the blocking layers at zero bias level. In the measurement of f_c, the laser was biased, when the middle *pn* junction was reverse-biased. Thus the depletion region was widened and the associated capacitance reduced, which might contribute to the increase in f_c.

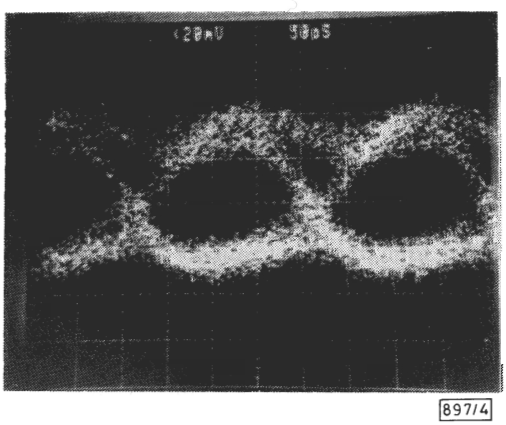

Fig. 4 *Eye pattern of modified DFB-PPIBH laser under 5 Gbit/s NRZ modulation*

Conclusion: The DFB-PPIBH laser cutoff frequency f_c was improved. An f_c of 4·3 GHz was obtained, which agreed exactly with f_c deduced from the fall time, and which agreed roughly with the calculated f_c. Under 5 Gbit/s NRZ modulation a good eye pattern was obtained.

Acknowledgment: We are grateful to Dr. W. Susaki of Mitsubishi Electric Corporation for his continuous encouragement and fruitful discussions.

S. KAKIMOTO
H. WATANABE
M. FUJIWARA
Y. OHKURA
Y. NAKAJIMA
Y. SAKAKIBARA

LSI R&D Laboratory
Mitsubishi Electric Corporation
4-1 Mizuhara, Itami, Hyogo 664, Japan

25th November 1988

References

1 BOWERS, J. E., TSANG, W. T., and KOCH, T. L.: 'Microwave intensity and frequency modulation of heteroepitaxial-ridge-overgrown distributed feedback lasers', *Appl. Phys. Lett.*, 1985, **46,** pp. 233–235

2 WÜNSTEL, K., MOZER, A., SCHILLING, M., LUZ, G., LÖSCH, K., SCHWEIZER, H., SCHEMMEL, G., and HILDEBRAND, O.: 'High-speed 1·3 μm DFB laser with modified DCPBH structure', *Electron. Lett.*, 1986, **22,** pp. 1144–1145

3 KIHARA, K., KAMITE, K., SUDO, H., TANAHASHI, T., KUSUNOKI, T., ISOZUMI, S., ISHIKAWA, H., and IMAI, H.: 'High-power, wide-bandwidth, 1·55 μm-wavelength GaInAsP/InP distributed feedback laser', *ibid.*, 1987, **23,** pp. 941–942

4 KAMITE, K., SUDO, H., YANO, M., ISHIKAWA, H., and IMAI, H.: 'Ultra-high speed InGaAsP/InP DFB lasers emitting at 1·3 μm wavelength', *IEEE J. Quantum Electron.*, 1987, **QE-23,** pp. 1054–1058

5 ISHIKAWA, H., SODA, H., WAKAO, K., KIHARA, K., KAMITE, K., KOTAKI, Y., MATSUDA, M., SUDO, H., YAMAKOSHI, S., ISOZUMI, S., and IMAI, H.: 'Distributed feedback laser emitting at 1·3 μm for gigabit communication systems', *J. Lightwave Technol.*, 1987, **LT-5,** pp. 848–854

6 TAKEMOTO, A., SAKAKIBARA, Y., NAKAJIMA, Y., FUJIWARA, M., KAKIMOTO, S., NAMIZAKI, H., and SUSAKI, W.: '1·3 μm InGaAsP/InP distributed-feedback *p*-substrate partially inverted buried-heterostructure laser diode', *Electron. Lett.*, 1987, **23,** pp. 546–547

RADIATION PATTERN OF PARABOLIC REFLECTOR ANTENNA FROM NEAR-FIELD MEASUREMENTS OF COUPLED REFLECTOR

Indexing terms: Antennas, Antenna radiation patterns, Reflector antennas

The presented scheme permits a more direct prediction of the radiation pattern of a parabolic reflector antenna.

Introduction: Considerable effort has been devoted to predicting the far-field gain and radiation pattern of antennas from near-field measurements.[1–3] More recently compact ranges[4] and modern digital techniques have been used to make these predictions to save on cost of a test site, to avoid interference from the surroundings, or to minimise the loss of information and measurement sensitivity which usually occurs in the far field. The scheme proposed here is inherited from geometrical optics[5,6] but is novel in that it permits a more direct prediction of the radiation pattern of a parabolic reflector antenna from an experimental plot of the electric field strength E_f over the focal region of a larger parabolic reflector in the near-field region of a test antenna. In this scheme, the parabolic reflector has a large f/D ratio, and its aperture is aligned with and faces the aperture of the test antenna at a separation distance nearly

equal to the diameter of the test antenna. Under this measurement condition, the distribution of the electric field strength in the focal region of the parabolic reflector is proportional to the Fourier transform of the aperture distribution of the test antenna. Using simple graphical rescaling, the desired far-field radiation pattern of the test antenna can be obtained.

Theory: Let the reflector R be placed in the near-field region of the test antenna T, as shown in Fig. 1, and let the separation distance between the two coupled aligned apertures be nearly equal to or less than the diameter of T. Based on geometrical optics and neglecting diffraction losses it can be assumed that the aperture field distribution $E(\rho, \phi)$ of the test antenna is incident on the aperture of R. This incident aperture field distribution can be expressed in terms of the reflector co-ordinate system, i.e. $E(\theta', \phi')$.

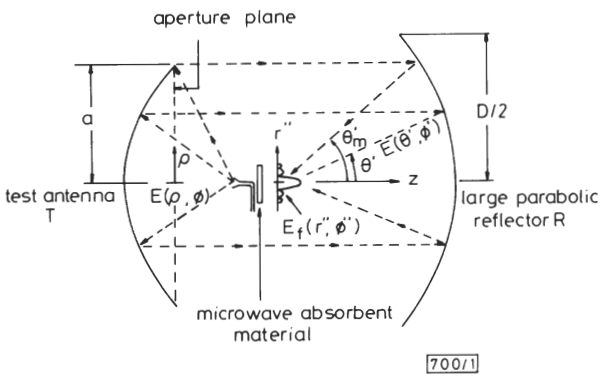

Fig. 1 *Schematic diagram of proposed experimental scheme*

Using this assumption, the electrical field distribution in the focal region of reflector R may be written as

$$E_f(r'', \phi'') \propto \int_0^{2\pi} \int_0^{\theta_m'} \frac{E(\theta', \phi')}{\cos^2(\theta'/2)} e^{jkr'' \sin\theta' \cos(\phi' - \phi'')} \sin\theta' \cos\theta' \, d\theta' \, d\phi' \tag{1}$$

where θ_m' is the maximum angle subtended by the incident aperture field at the focus of reflector R, as shown in Fig. 1. Note that we have employed two polar co-ordinate systems (ρ, ϕ) for the aperture of T and (r'', ϕ'') for focal region of R plus the two spherical co-ordinate systems (r, θ, ϕ''') and (r', θ', ϕ'), centred at the midpoints of each aperture plane of T and R, respectively.

Letting $S_m = \sin\theta_m'$, $S' = \sin\theta'/S_m$, we can rewrite eqn. 1 in the form

$$E_f(r'', \phi'') \propto S_m^2 \int_0^{2\pi} \int_0^{1} \frac{E(\theta', \phi')}{\cos^2(\theta'/2)} e^{jkr''S'S_m \cos(\phi' - \phi'')} S' \, dS' \, d\phi' \tag{2}$$

For a large f/D ratio of the reflector R, the angle subtended by the refocused signal is quite small, therefore, the tapering function $\cos^2(\theta'/2)$ is approximately equal to unity and eqn. 2 hence becomes

$$E_f(r'', \phi'') \propto S_m^2 \int_0^{2\pi} \int_0^{1} E(\theta', \phi') e^{jkr''S'S_m \cos(\phi' - \phi'')} S' \, dS' \, d\phi' \tag{3}$$

The radiation pattern of the test antenna can be expressed as the Fourier transform of the aperture field distribution $E(\rho, \phi)$, i.e.

$$E_r(s, \phi''') \propto \int_0^{2\pi} \int_0^{1} E(\rho, \phi) e^{jkus \cos(\phi' - \phi''')} u \, du \, d\phi \tag{4}$$

where $u = \rho/a$, $s = a \sin\theta$ and a is the aperture radius of the antenna under test.

By comparing eqns. 3 and 4, it is obvious that eqn. 4 can be obtained from eqn. 3 simply by interchanging the parameters as follows:

Eqn. 3		Eqn. 4
$r''S_m$	→	s
S'	→	u
ϕ'	→	ϕ

It is to be noted that eqns. 3 and 4 in fact represent the Fourier transform of the same function E which is expressed in terms of the co-ordinates (ρ, ϕ) and (θ', ϕ'). Thus, a measurement of the field distribution $E_f(r'', \phi'')$ in the focal region of R yields the desired radiation pattern of T. To yield the radiation pattern, E_f should first be plotted against r'' at $\phi'' = 0, \pi/2$ (i.e. along both principal planes). Since $r'' = a \sin\theta/\sin\theta_m'$, it follows that

$$\theta = \sin^{-1}[r'' \sin\theta_m'/a] \tag{5}$$

and the E_f against r'' experimental plot can be reached to yield the desired far-field pattern E against θ using eqn. 5 where the maximum value of θ cannot exceed θ_m'.

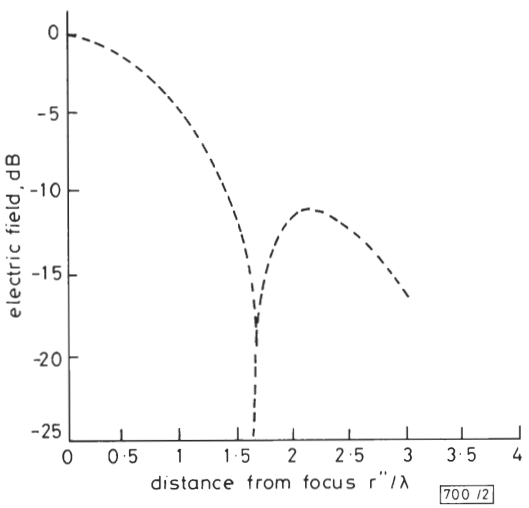

Fig. 2 *E-plane electric field distribution in focal region of reflector R*

A factor that must be taken into account in the proposed scheme is the error caused by blockage and scattering of the electric field by the probe during the measurement of the radiation pattern. This problem can be overcome by using an offset reflector which focuses the reflected wave to the focal point outside the propagating zone, as shown in Fig. 2. It should be noted that for a large f/D ratio, the electric field distribution in the focal region of an offset reflector is almost the same as that of a symmetrical paraboloid with an equivalent focal length f[7,8] where

$$f' = \frac{2f}{1 + \cos\phi_0}$$

This concept was also presented in the 1988 IEEE AP-S international symposium.[9]

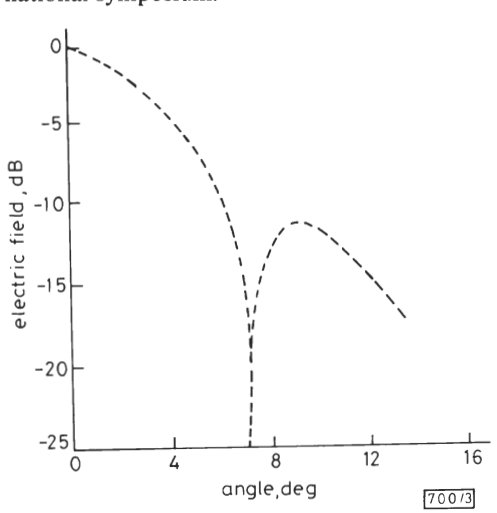

Fig. 3 *Radiation pattern of test antenna obtained by rescaling of field plot of Fig. 2*

Experimental results and conclusions: The proposed scheme for a centre-fed parabolic dish antenna was verified experimentally at 10 GHz for a test antenna of 60 cm (2 ft) diameter and f/D ratio of 0·4. The reflector diameter was 120 cm (4 ft) with $\theta_m = 14°$ and an f/D ratio of 1·05. The separation distance from focus to focus was 22·5 cm (9″) while the probe used to measure $|E_f|$ was a Hertzian dipole on a sliding mechanism and with a metal reflector in the back to avoid receiving any signals from the test antenna. The open-ended waveguide feed of the test antenna was similarly shielded from reradiation by T through a thin sheet of microwave absorber.

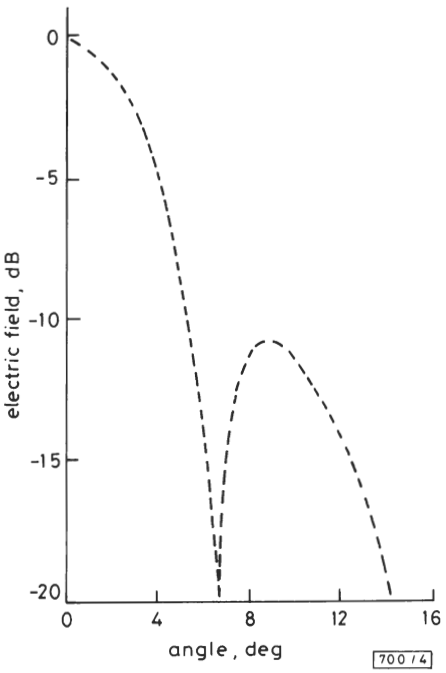

Fig. 4 *Measured far-field radiation pattern of test antenna T*

The experimental plot of E_f against r''/λ in the E-plane is limited for practical reasons (since θ'_m of reflector R was restricted to 14°) to the main and first sidelobes as shown in Fig. 3. Using the proposed scheme, E_f is rescaled to yield the desired radiation pattern of the test antenna shown in Fig. 4 (solid line). This radiation pattern compares favourably with the experimental far-field radiation pattern of the test antenna, also shown in Fig. 4 (dashed line), obtained by the usual far-field measurement technique. Work pertaining to the degree of resolution of the proposed scheme is under investigation. The results indicate that the scheme can be set-up with reasonable accuracy allowing for diffraction and tapering function approximation.

M. HOQUE

Bell Communications Research Inc.
Morristown, NJ 07960, USA

M. HAMID

Department of Electrical Engineering
University of Central Florida
Orlando, FL 32816, USA

A. RAHMAN

Department of Electrical Engineering
Bangladesh University of Electrical Engineering
Dacca, Bangladesh

A. Z. ELSHERBENI

Department of Electrical Engineering
University of Mississippi
MS 38677, USA

27th October 1988

References

1 BROWN, J., and JULL, E. V.: 'The prediction of aerial radiation pattern from near-field measurements', *Proc. IEE*, 1961, **108c,** pp. 635–644
2 HAMID, M.: 'The radiation pattern of an antenna from near-field correlation measurements', *IEEE Trans.*, 1968, **AP-16,** (3), pp. 351–353
3 CHU, T. S., and SEMPLAK, R. A.: 'Gain of electromagnetic horns', *Bell Syst. Tech. J.*, 1965, **64,** (3), pp. 527–537
4 HOQUE, M., SMITH, M. S., and DAVIES, D. E. N.: 'Compact gain measurements on reflector antennas', *IEE Proc. H, Microwaves, Antennas & Propag.*, 1984, **131,** (6), pp. 371–378
5 SILVER, S.: 'Microwave aperture antennas and diffraction theory', *J. Opt. Soc. Am.*, 1962, **52,** (2), pp. 131–139
6 KENNAUGH, E. M., and OTT, R. H.: 'Fields in the focal region of parabolic receiving antennas', *IEEE Trans.*, 1964, **AP-12,** pp. 370–377
7 BEM, D. J.: 'Electric field distribution in the focal region of an offset paraboloid', *IEEE Proc.*, 1960, **116,** (5), pp. 679–684
8 VENTINO, A. R., and TONLIOUS, P.: 'Fields in the focal region of offset parabolic antennas', *IEEE Trans.*, 1976, **AP-24,** pp. 859–865
9 HOPE, M., *et al.*: 'Radiation pattern of a parabolic reflector antenna from near-field measurement of a coupled reflector'. IEEE AP-S International Symposium, 1988, **3,** pp. 1110–1113

Erratum

CHENG, Y. H., and LIN, W. G.: 'Local field in a bent step index fibre', *Electron. Lett.*, 1988, **24,** (6), pp. 332–333

Eqn. 7 should read

$$u\bar{x}_m^2\left(\frac{J_0}{J_1}\right)\left[\left(\frac{J_0}{J_1}\right)^2 + 2\right] - 3\left(\frac{J_0}{J_1}\right)^2 \bar{x}_m + \frac{u^2}{(\beta^{(0)}a)^2}\frac{R}{a} = 0$$

In the first line below Fig. 2, $\tilde{E}_y = E_y/J_0(u)$ should be $\tilde{E}_y = E_y \cdot J_0(u)$

The letter 'R' in Fig. 3 should be '$\mathscr{R}$'